Evaluating the effect of PD-1 inhibitors on left ventricular function in lung cancer with noninvasive myocardial work

Xia Li[1,2#]^, **Chujun Wang**[1#]^, **Ruirui Kang**[1#], **Yu Zhao**[1]^, **Lili Chen**[1], **Fengzhen Liu**[1], **Xiaolin Wang**[1], **Yulan Peng**[1], **Chunquan Zhang**[1]^

[1]Department of Ultrasound, the Second Affiliated Hospital of Nanchang University, Nanchang, China; [2]Department of Ultrasound, Ganzhou People's Hospital, Ganzhou, China

Contributions: (I) Conception and design: All authors; (II) Administrative support: C Zhang, Y Peng; (III) Provision of study materials or patients: C Zhang, C Wang, R Kang; (IV) Collection and assembly of data: X Li, Y Zhao, L Chen, F Liu, X Wang; (V) Data analysis and interpretation: X Li, C Wang, R Kang, Y Peng; (VI) Manuscript writing: All authors; (VII) Final approval of manuscript: All authors.

[#]These authors contributed equally and should be regarded as co-first authors.

Correspondence to: Chunquan Zhang. Department of Ultrasound, the Second Affiliated Hospital of Nanchang University, No. 1, Minde Road, Donghu District, Nanchang 330006, China. Email: jxzcq@163.com.

Background: The treatment of advanced lung cancer has been revolutionized by immune checkpoint inhibitors (ICIs) in recent years, largely driven by programmed cell death-1 (PD-1) inhibitors. However, patients with lung cancer who are treated with PD-1 inhibitors are prone to immune-related adverse events (irAEs), especially cardiac adverse events. Noninvasive myocardial work is a novel technique used to assess left ventricular (LV) function, which can effectively predict myocardial damage. Here, noninvasive myocardial work was used to evaluate changes in LV systolic function during PD-1 inhibitor therapy and to assess ICIs-related cardiotoxicity.

Methods: From September 2020 to June 2021, 52 patients with advanced lung cancer in the Second Affiliated Hospital of Nanchang University were prospectively enrolled. In total, 52 patients underwent PD-1 inhibitor therapy. The cardiac markers, noninvasive LV myocardial work, and conventional echocardiographic parameters were measured at pretherapy (T0) and posttreatment after the first (T1), second (T2), third (T3), and fourth (T4) cycles. Following this, the trends of the above parameters were analyzed using analysis of variance with repeated measures and the Friedman nonparametric test. Furthermore, the relationships between disease characteristics (tumor type, treatment regimen, cardiovascular risk factors, cardiovascular drugs, and irAEs) and noninvasive LV myocardial work parameters were assessed.

Results: Throughout the follow-up, the cardiac markers and conventional echocardiographic parameters showed no significant changes. Based on the normal reference ranges, patients with PD-1 inhibitor therapy had increased values of LV global waste work (GWW) and decreased global work efficiency (GWE) that began at T2. Compared with T0, GWW increased from T1 to T4 (42%, 76%, 87%, and 87%, respectively), while global longitudinal strain (GLS), global work index (GWI), and global constructive work (GCW) decreased in varying degrees ($P<0.001$). Most of the disease characteristics had no effect on the LV myocardial work parameters; however, the numbers of irAEs were closely associated with GLS ($P=0.034$), GWW ($P<0.001$), and GWE ($P<0.001$). Patients with 2 or more irAEs had higher values of GWW and lower GLS and GWE.

Conclusions: Noninvasive myocardial work can accurately reflect myocardial function and energy utilization in patients with lung cancer who are undergoing PD-1 inhibitor treatment and may thus benefit the management of patients with ICIs-related cardiotoxicity.

Keywords: Lung cancer; PD-1 inhibitor; left ventricular function; echocardiography; myocardial work

Introduction

Lung cancer is the malignant tumor with the highest incidence and mortality rate worldwide (1). Despite the availability of neoadjuvant chemotherapy, surgical treatment, and adjuvant therapy, the prognosis for patients with advanced lung cancer remains poor (2). Immune checkpoint inhibitors (ICIs) have revolutionized cancer treatment, and studies have shown that ICIs significantly improve the long-term survival rate of those with advanced lung cancer (3,4). Among ICIs, programmed cell death-1 (PD-1) inhibitors and programmed cell death ligand-1 (PD-L1) inhibitors are important components in the field of immunotherapy.

However, ICIs can lead to a series of immune-related adverse events (irAEs), which affect almost all organs and systems of the body. Involvement of the cardiovascular system mainly affects cardiac conduction and cardiomyocyte function, which manifests as myocarditis, myocardial fibrosis, arrhythmia, pulmonary hypertension, vasculitis, and atherosclerosis (5-7). With the increasing application of ICIs, the incidence of cardiac adverse events (CAEs) appears to be rising. Studies have shown that in patients being treating with PD-1 inhibitors, the incidence of CAEs is 16%, and the mortality rate of ICIs-related myocarditis is as high as 53% (8,9). In addition, the relative rate of CAEs is higher in patients with lung cancer treated with PD-1 inhibitors (10). Accordingly, early detection of ICIs-related CAEs is essential to preventing irreversible cardiac dysfunction and reducing mortality and morbidity.

Cancer treatment-related cardiac dysfunction is usually defined as a decline in the left ventricular ejection fraction (LVEF) (11). Speckle tracking echocardiography (STE) has been widely used to detect cardiac injury and to predict CAEs during cytotoxic drug chemotherapy (12-14). Nevertheless, both LVEF and STE are load dependent, which may lead to an underestimation of the true myocardial systolic function (15). Recently, Russell *et al.* (16) proposed noninvasive myocardial work as an assessment which improves upon the analysis of cardiac load dependence-based on STE via the construction of a pressure–strain loop involving the combination of LV strain and pressure. Noninvasive myocardial work has recently been used to evaluate the effect of cardiac resynchronization therapy on coronary heart disease and primary cardiomyopathy (17). This technique has not yet been applied to measure cardiac function in patients receiving ICIs. Therefore, in this study, noninvasive myocardial work was used to evaluate changes in LV systolic function during PD-1 inhibitor therapy and to assess ICIs-related cardiotoxicity. We present the following article in accordance with the STROBE reporting checklist (available at https://qims.amegroups.com/article/view/10.21037/qims-22-817/rc).

Methods

Study population and data collection

Between September 2020 and June 2021, potentially eligible patients with advanced lung cancer were prospectively enrolled in the Second Affiliated Hospital of Nanchang University. All patients underwent PD-1 inhibitor therapy or combined chemotherapy. The exclusion criteria were as follows: (I) patients with diseases affecting cardiac function, (II) patients with abnormal electrocardiography (ECG) or echocardiogram before treatment, (III) patients who had previously undergone radiotherapy or anthracycline chemotherapy, (IV) patients receiving glucocorticoids during treatment, and (V) patients with important clinical information missing (*Figure 1*). The study was conducted in accordance with the Declaration of Helsinki (as revised in 2013) and was approved by the Ethics Committee of the Second Affiliated Hospital of Nanchang University (No. 20220718034425258). Informed consent was obtained from all participants.

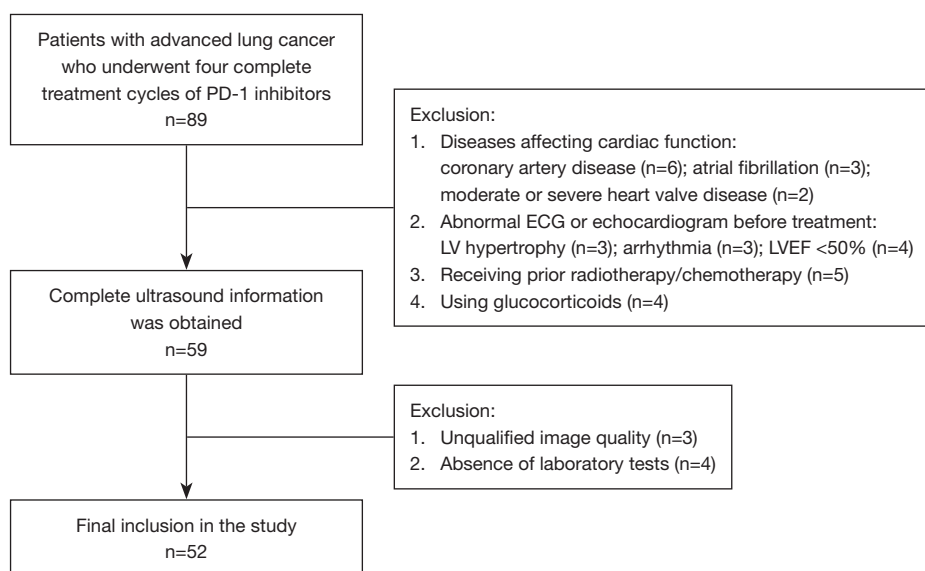Based on previous studies concerning ICIs-related

Figure 1 The flowchart of the study with inclusion and exclusion criteria. ECG, electrocardiography; LV, left ventricle; LVEF, left ventricular ejection fraction; PD-1, programmed cell death-1.

CAEs, the average variation of LVEF after intervention was 4.15% (18). SPSS version 15.0 (IBM Corp.) estimated that the minimum sample size was 37. This minimum sample size was based on an inspection level of 0.05, a power of a test of 0.8, an autocorrelation coefficient of 0.2, 5 repeated measurements, and a missing rate of 20%.

The drugs used were camrelizumab (200 mg), pembrolizum (200 mg), carboplatin 400 mg/m^2, and paclitaxel 150 mg/m^2, which were administered via an intravenous drip once every 21 days. The recognized high-risk time window for ICIs-related CAEs is within 90 days after treatment initiation (19,20). Therefore, before patients underwent PD-1 inhibitor therapy (T0) and after the first (T1), second (T2), third (T3), and fourth (T4) cycles, all patients underwent electrocardiography, laboratory testing, and standard transthoracic echocardiography within 72 hours.

The cardiac markers were measured, including creatine kinase (CK; 0–310 U/L), creatine kinase isoenzyme (CK-MB; 2–25 U/L), lactate dehydrogenase (LDH; 120–250 U/L), ultrasensitivity troponin I (TnI-Ultra; 0–0.78 μg/L), and B-type natriuretic peptide (BNP; 0–100 pg/mL). The numbers in parentheses refer to the normal reference ranges (21). The demographic and clinical data of the patients were recorded.

Echocardiographic analysis

Transthoracic echocardiography examinations were performed by a radiologist with over 5 years of work experience in echocardiography. All patients were examined using the Vivid E95 ultrasound system (GE Vingmed Ultrasound AS) equipped with the 3.5-MHz electronic transducer. The measurements were collected in accordance with the guidelines of the American Society of Echocardiography and the European Association for Cardiovascular Imaging (22).

The end-systolic left atrial diameter (LAD), the end-diastolic interventricular septum thickness, and LV posterior wall thickness were measured on the parasternal long-axis section. The LV end-diastolic (LVEDV), LV end-systolic volumes (LVESV), and LVEF were measured from the apical 4- and 2-chamber views using the Simpson biplane method. In the apical 4-chamber view, mitral peak early diastolic velocity (E) and peak late diastolic velocity (A) were measured with a pulsed wave Doppler. The septal velocity (e') was measured with tissue Doppler imaging, which showed the average value of early peak velocity of the septal and lateral annuli. The ratios of E/A and E/e' were calculated.

Quantification of LV myocardial work

All participants assumed the left lateral position and had placid breathing. Their brachial artery pressure was measured (as the average value of 3 measurements) while connected to the ECG. Then, images of apical 2-chamber,
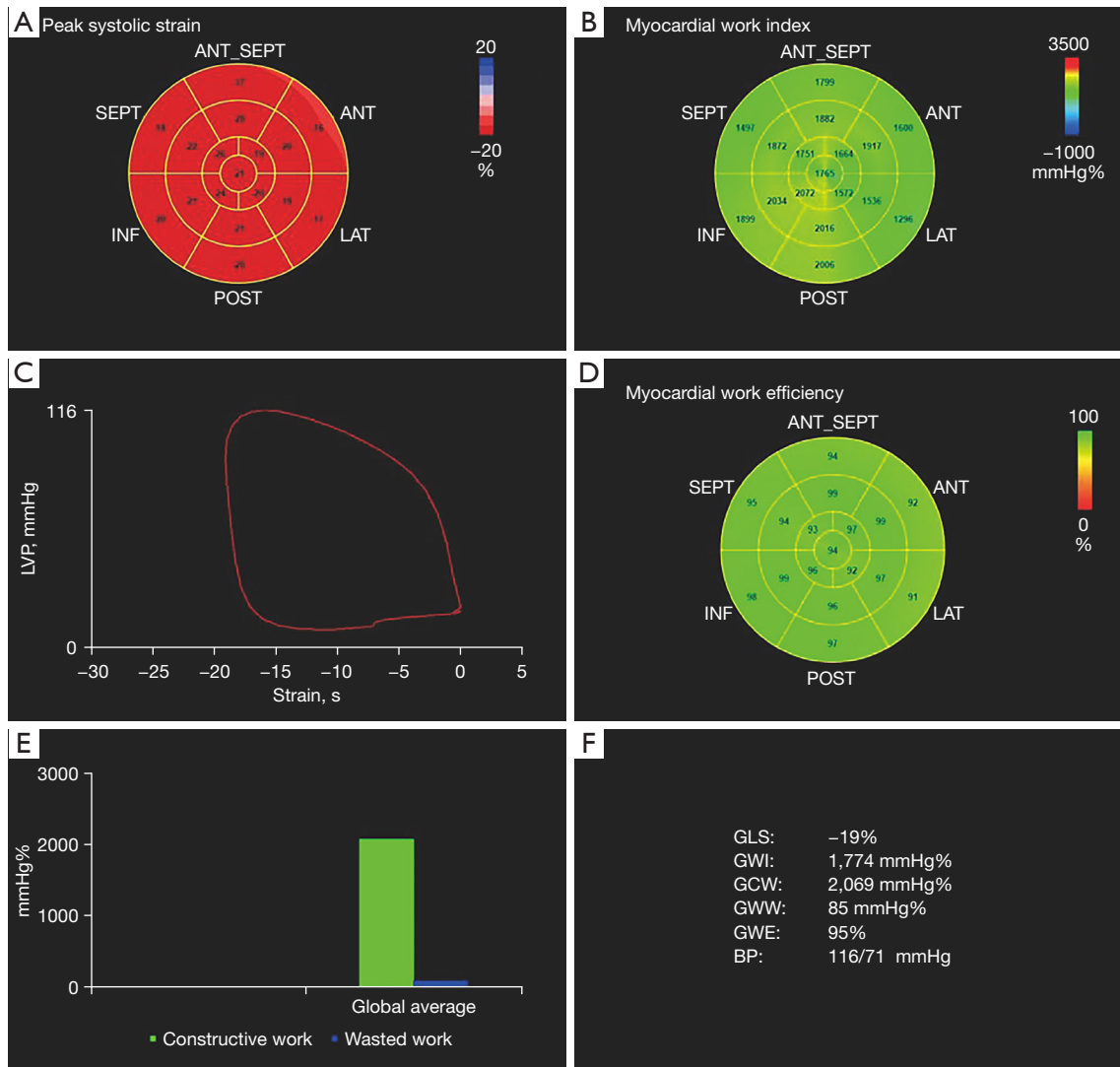
Figure 2 The analysis of LV myocardial work. (A and B) The left side is the bullseye plot of 17 segments, which shows GLS, while the right side shows GWI. (C) The pressure-strain loop, with the area representing GWI. (D) The GWS. (E) The GCW (green column) and GWW (blue column). (F) The specific values of the parameters. ANT, anterior; SEPT, septal; INF, inferior; LAT, lateral; POST, posterior; BP, blood pressure; LV, left ventricle; GLS, global longitudinal strain; GWI, global work index; GCW, global constructive work; GWE, global work efficiency; GWW, global waste work; LVP, left ventricular pressure.

3-chamber, and 4-chamber views of at least 3 cardiac cycles were digitally stored at a speed of 40–80 frames per second. In order to obtain clearly visible endocardial boundaries throughout the cardiac cycle, participants were encouraged to adjust their breathing during the acquisition.

Analysis of the images was completed offline on dedicated software (EchoPAC PC version 203; GE Healthcare). The 3-, 4-, and 2-chamber views were selected in turn using the automated function imaging mode. The software automatically sketched the endocardial and

epicardial boundaries to form regions of interest, and these were manually adjusted to include the entire myocardial thickness. The system automatically analyzed the 17 LV segments as well as the global longitudinal strain (GLS) and peak strain dispersion (PSD) of the LV.

The apical 3-chamber view was used to identify the openings and closures of mitral and aortic valves to define the duration of isovolumic contraction, ejection, and isovolumic relaxation (23,24). Subsequently, the following myocardial work parameters were generated with the software (*Figure 2*):

(I) LV global work index (GWI; mmHg%)—the total work of the LV during a cardiac cycle; (II) LV global constructive work (GCW; mmHg%)—the work of the function of lengthening during diastole and shortening during systole; (III) LV global wasted work (GWW; mmHg%)—the work of LV myocardial lengthening/shortening that does not occur in the appropriate cardiac phase; and (IV) LV global work efficiency (GWE; %)—the comprehensive estimation of LV performance calculated as [GCW/(GCW + GWW)] × 100%—which reflects the efficiency of energy expended during the cardiac cycle.

Statistical analysis

The normality of measurement data was evaluated using histograms and P-P plots. Normally distributed continuous variables are presented as the mean ± standard Deviation. Nonnormally distributed data are displayed as the median and interquartile range. Categorical variables are expressed as frequencies and percentages. Comparison of measured parameters and percentage changes during T0 to T4 were tested using one-way analysis of variance (ANOVA; for normally distributed continuous variables) and the Friedman nonparametric test (for nonnormally distributed continuous variables). Fifteen random patients were selected for repeated measurements, and the intra- and interobserver variability of myocardial work indices were analyzed using the intra-class correlation coefficient (ICC). Excellent agreement was defined as an ICC >0.9, whereas good agreement was defined as an ICC between 0.75 and 0.90 (25).

The interactions between disease characteristics and treatment cycles were calculated with one-way ANOVA with repeated measurements. Specifically, the disease characteristics included tumor type (2 groups: squamous cell carcinoma and adenocarcinoma), treatment regimen (3 groups: PD-1 inhibitor + paclitaxel, PD-1 inhibitor + platinum, and PD-1 inhibitor), cardiovascular risk factors (3 groups: 0, 1, and 2), cardiovascular drugs (2 groups: yes and no), and irAEs (4 groups: 0, 1, 2, and 3). For instance, when the interaction between the tumor type and treatment cycle under PSD was examined, the group of the tumor type was adopted as a between-subjects factor, the treatment cycle was adopted as a within-subject factor, and T0 to T4 were adopted as within-subjective variables. First, the experimental results were interpreted with the Mauchly's sphericity test. If P>0.05, the result was followed by tests of within-subjects effects. Then, when the table of the test was

viewed, if P<0.05, the result was considered to show that the treatment cycle could affect the value of PSD and that there was a significant interaction between the treatment cycle and tumor type. As time went on, these findings suggested that the effect of tumor type on PSD was statistically significant. Finally, when the table of tests of between-subjects effects was viewed, if P<0.05, the tumor type under PSD significantly differed, and the values of F and P were recorded. All tests were two-sided, and a P value <0.05 was considered statistically significant. Statistical analyses were processed using SPSS version 25.0 (IBM Corp.).

Results

Patients characteristics

From September 2020 to June 2021, this study prospectively recruited 89 patients with advanced lung cancer who underwent 4 complete cycles of PD-1 inhibitor therapy. Among these patients, 37 patients were excluded. Finally, 52 patients were enrolled for analysis (*Figure 1*).

Among the 52 patients, there were 37 males (37/52, 71%) and 15 females (15/52, 29%). The mean age was 62.73±9.18 years old, and the mean body surface area was 1.67±0.13 m². The final pathologic diagnosis demonstrated that 34 patients had squamous cell carcinoma (34/52, 65%) and 18 had adenocarcinoma (18/52, 35%). After receiving PD-1 inhibitor therapy (30 camrelizumab and 22 pembrolizum), patients developed various irAEs, including fatigue, dermatitis, gastrointestinal symptoms, hepatitis, thyroiditis, arthritis, and other symptoms. In the follow-up to the end of 4 cycles, there were 10 cases with 1 irAE, 8 cases with 2 irAEs, and 3 cases with 3 irAEs. The detailed baseline characteristics are shown in *Table 1*.

Clinical data and standard echocardiographic parameters

There were no significant changes in cardiac markers, blood pressure, heart rate, or ventricular chamber size throughout the follow-up. When differences between multiple groups were compared, the P values of BNP and LVEDV were 0.030 and 0.024, respectively. After being corrected by the Bonferroni method, there were no significant differences in the pairwise comparison (P>0.05). *Table 2* shows that the results of CK, CK-MB, LDH, and BNP were in the reference range. Compared with T0, these markers all fluctuated at varying degrees from T1 to T4. Furthermore, the LVEF was >50% in all patients.

Table 1 Baseline characteristics of the study population

Variables	Population (n=52)
Clinical and demographic characteristic	
Median age, years	62.73±9.18
Median body surface area, m²	1.67±0.13
Sex, male	37 (71%)
Histologic type	
Squamous cell carcinoma	34 (65%)
Adenocarcinoma	18 (35%)
Treatment regimen	
PD-1 inhibitor + paclitaxel	11 (21%)
PD-1 inhibitor + platinum	13 (25%)
PD-1 inhibitor	28 (54%)
Cardiovascular risk factor	
Hypertension	8 (15%)
Hyperlipemia	6 (12%)
Smoking history	15 (29%)
Cardiovascular drug	
Angiotensin-converting enzyme inhibitor	6 (12%)
Calcium channel blocker	4 (8%)
β-blocker	2 (4%)
Statins	6 (12%)
irAE	
Fatigue	8 (15%)
Dermatitis	14 (27%)
Gastrointestinal symptoms	4 (8%)
Hepatitis	2 (4%)
Thyroiditis	4 (8%)
Arthritis	2 (4%)

Values are presented as the mean ± standard deviation (continuous data) or numbers (%) (categorical data). irAE, immune-related adverse event; PD-1, programmed cell death-1.

Myocardial work analysis

Figure 3 shows the trends of the myocardial work indices. Compared with T0, PSD increased (F=9.876; P<0.001) and GLS decreased (F=13.611; P<0.001) after patients underwent PD-1 inhibitor therapy. These changes were more obvious during T1 and T2 and remained significant during T3 and T4 (PSD: 13% for T1, 18% for T2, 18% for T3, 20% for T4; GLS: 4% for T1, 6% for T2, 6% for T3, 7% for T4).

Table 3 summarizes the results of the myocardial work indices. These results revealed that the main change was in the growth of GWW (F=29.851; P<0.001). Compared with T0, the GWW increased by 42%, 76%, 87%, and 87% from T1 to T4, respectively. Meanwhile, GWI, GCW, and GWE decreased (F=25.668, F=19.233, and F=44.913, respectively; P<0.001), largely driven by T1 and T2. Compared with T0, GWI, GCW, and GWE decreased by 13%, 12%, and 4%, respectively, during T2. Based on the comparison with reported reference ranges (26,27), patients who underwent PD-1 inhibitor therapy had increased values of LV GWW and GWE beginning with T2. PSD, GLS, GWI, and GWE were maintained within the normal levels from T1 to T4.

The ICCs for the intraobserver variability of LV myocardial work indices were 0.954 for LV GWI, 0.990 for GCW, 0.965 for GWW, and 0.952 for GWE, demonstrating excellent agreement. The ICCs for the interobserver variability were 0.937 for LV GWI and 0.961 for GCW, 0.982 for GWW, and 0.979 for GWE, indicating excellent repeatability (*Table 4*).

Associations between disease characteristics and myocardial work indices

The results of tests of between-subjects effects are shown in *Table 5*. The effects of tumor type, treatment regimen, cardiovascular risk factors, and cardiovascular drugs on myocardial work indices showed no statistical significance (P>0.05). Notably, there were significant differences among irAEs on the basis of GLS, GWW, and GWE (P=00.034, P<0.001, and P<0.001, respectively), indicating that different numbers of irAEs may cause different variation tendencies of GLS, GWW, and GWE. When the number of treatment cycles increased, the effect of irAEs on GLS, GWW, and GWE showed statistical significance (both P values <0.05). *Table 6* shows the influences of irAEs on the changes of GLS, GWW, and GWE. When patients had 2 or 3 irAEs, the above indices were no longer at the normal reference range during T1 or T2.

Based on the above analysis, we further explored the relationships between treatment cycles and patients with different numbers of irAEs (*Figure 4*). From T1 to T4, compared with patients with 0 or 1 irAE, GLS and GWE decreased and GWW increased significantly in patients with 3 irAEs. During T2, compared with patients with

Table 2 Clinical data and standard echocardiographic parameters

Variables	T0	T1	T2	T3	T4	F/Z	P value
CK, U/L	72.49±36.35	76.42±36.50	75.95±48.29	82.61±61.18	75.64±54.57	2.149	0.089
CK-MB, U/L	15.24±4.71	16.22±7.03	16.63±6.28	15.56±4.90	15.16±4.38	2.544	0.051
LDH, U/L	164.94±32.75	174.25±31.41	162.99±28.51	166.80±31.17	172.96±36.43	2.297	0.073
TnI-Ultra, µg/L	0.01 [0.01–0.018]	0.01 [0.01–0.020]	0.01 [0.01–0.018]	0.01 [0.01–0.012]	0.01 [0.01–0.020]	1.994	0.737
BNP, µg/L	62.01±36.83	79.50±57.74	78.69±52.92	74.78±53.63	70.91±52.12	2.930	0.030
SBP, mmHg	122.06±13.95	121.17±12.93	117.10±12.44	117.38±12.54	119.50±12.94	2.353	0.055
DBP, mmHg	77.60±8.99	75.73±10.95	75.04±9.28	76.65±9.94	75.52±9.94	0.801	0.531
HR, beats/min	81.31±12.71	82.86±11.31	82.85±12.05	83.08±11.08	83.19±11.00	1.530	0.208
LAD, mm	31.65±2.24	31.96±2.01	31.83±2.08	31.65±2.20	31.71±2.28	2.063	0.100
IVS, mm	10 [9–10]	10 [9–10]	10 [9–10]	10 [9–10]	10 [9–10]	4.833	0.305
LVPW, mm	9 [9–10]	9 [9–10]	9 [9–10]	9 [9–10]	9 [9–10]	7.016	0.135
LVEDV, mL	98.00±6.40	98.42±6.38	99.17±6.33	98.60±3.86	99.71±4.63	3.033	0.024
LVESV, mL	36.27±5.57	36.54±5.74	36.88±5.70	37.06±4.81	37.00±4.89	2.262	0.076
LVEF, %	63.06±5.16	62.88±5.32	62.86±5.18	62.48±4.82	62.90±4.62	1.679	0.168
E/A	1.26 [0.79–0.65]	1.23 [1.11–1.36]	1.32 [1.13–1.42]	1.31 [1.18–1.42]	1.31 [1.18–1.45]	1.861	0.761
E/e'	9.08 [8.06–10.31]	8.97 [8.13–10.17]	9.45 [8.32–10.70]	9.54 [8.32–10.70]	9.79 [8.67–11.29]	4.891	0.398

Continuous values are presented as the mean ± standard deviation (normally distributed) or median [range; nonnormally distributed]. CK, creatine kinase; CK-MB, creatine kinase isoenzymes; LDH, lactic dehydrogenase; TnI-Ultra, ultrasensitivity troponin I; BNP, B-type natriuretic peptide; SBP, systolic blood pressure; DBP, diastolic blood pressure; HR, heart rate; LAD, left atrial diameter; IVS, interventricular septum; LVPW, left ventricular posterior wall thickness; LVEDV, left ventricular end-diastolic and end-systolic volume; LVEF, left ventricular ejection fraction; E, mitral peak early diastolic velocity; A, mitral peak late diastolic velocity; e', the septal velocity; LVESV, left ventricular end-systolic volumes.
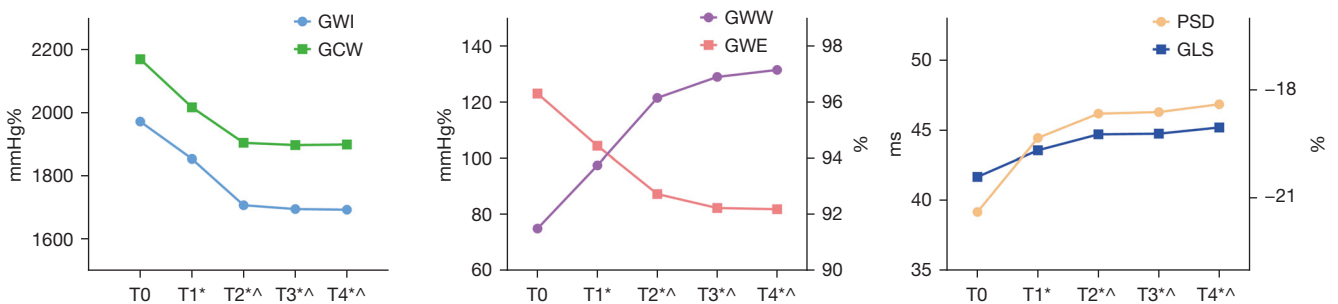

Figure 3 The trends of myocardial work indices in patients with lung cancer during PD-1 inhibitor therapy. *, the difference is statistically significant compared with T0; ^, the difference is statistically significant compared with T1. PD-1, programmed cell death-1; PSD, peak strain dispersion; GLS, global longitudinal strain; GWI, global work index; GCW, global constructive work; GWW, global wasted work; GWE, global work efficiency.

2 irAEs, patients with 3 irAEs had a greater reduction in GWE and an increase in GWW. During T4, compared with patients with 0 or 1 irAE, patients with 2 irAEs had a greater reduction for GWE and an increase in GWW.

Discussion

In this study, noninvasive myocardial work was used to evaluate LV systolic function in patients with lung cancer

Table 3 Myocardial work indices

Variables	Baseline	T0	T1	Δ%	T2	Δ%	T3	Δ%	T4	Δ%	F	P value
PSD, ms	38.4±9.6	39.17±5.14	44.44±7.97†	13	46.17±8.63†	18	46.29±8.75†	18	46.85±8.95†	20	9.876	<0.001
GLS, %	−18.4±3.0	−20.40±1.18	−19.67±1.59†	4	−19.23±1.7§†	6	−19.21±1.68†‡	6	−19.04±1.66†‡	7	13.611	<0.001
GWI, mmHg%	2084±483	1969.67±222.05	1837.29±169.07†	7	1704.96±124.73†‡	13	1694.94±145.82†‡	14	1692.88±136.62†‡	14	25.668	<0.001
GCW, mmHg%	2082±525	2168.88±264.87	2016.44±162.30†	7	1903.85±180.24†‡	12	1897.04±188.29†‡	13	1898.62±152.77†‡	12	19.233	<0.001
GWW, mmHg%	116±61	78.08±19.05	110.85±42.90†	42	137.08±39.24†‡	76	145.71±55.40†‡	87	146.23±48.06†‡	87	29.851	<0.001
GWE, %	94.4±2.6	96.31±1.09	94.44±2.12†	2	92.73±2.25†‡	4	92.23±3.25†‡	4	92.19±2.47†‡	4	44.913	<0.001

Data are presented as the mean ± standard deviation. Δ%, percentage change from baseline; †, The difference was statistically significant compared with T1; ‡, The difference was statistically significant compared with T0; PSD, peak strain dispersion; GLS, global longitudinal strain; GWI, global work index; GCW, global constructive work; GWW, global wasted work; GWE, global work efficiency.

who were treated with PD-1 inhibitors. We found that myocardial work indices changed after 1 cycle of therapy. Specifically, GLS, GWI, GCW, and GWE all decreased to varying degrees, while PSD and GWW increased. At the end of 4 cycles, GWW and GWE were not in the normal reference range, and the above trends were more obvious during T1 and T2 than during T3 and T4. Conversely, conventional echocardiography and cardiac markers did not show any significant changes during the follow-up. The associations between disease characteristics and myocardial work indices were explored. The cardiac function of patients with 2 or 3 irAEs changed more obviously, and GLS, GWW, and GWE were no longer in the normal reference range during T1 or T2. Furthermore, there was no significant interactions between tumor type, treatment regimen, cardiovascular risk factors, cardiovascular drugs, and myocardial work indices.

The underlying pathophysiological mechanisms of immune-mediated CAEs remain unclear. The mechanism is speculated to be related to the sharing of T-cell targeting antigens among the tumor, skeletal muscle, and myocardium. During the treatment, immune response–activated T cells recognize antigens on the surface of cardiac myocytes, leading to myocardial cell injury. However, there are no evidence-based guidelines for screening and monitoring ICIs-related CAEs because of the lack of prospective trials and clinical monitoring tools. Our results suggest that noninvasive myocardial work may be applied to the monitoring of ICIs-related CAEs. Myocardial work indices begun to change from T1 to T2, and GWW and GWE were no longer in the normal reference range from T3 to T4, indicating that LV systolic function was impaired. The onset time of ICIs-related CAEs is early, the majority occurs in the first 3 months of treatment (28), 76% occurs in the first 6 weeks (29), and 79% of patients with CAEs develop LV systolic dysfunction (20,30). Previous studies have demonstrated that the PD-1 pathway hinders tissue inflammation and cardiomyocyte injury (31). Preclinical animal models of myocarditis have found that PD-1 gene–deficient mice produce high titers of cardiac troponin I–specific antibody, leading to severe LV systolic dysfunction and congestive heart failure (32).

In this study, PD-1 inhibitors, PD-1 inhibitors + paclitaxel and PD-1 inhibitors + platinum were included in the treatment regimens, and no effect of different treatment regimens on myocardial work indices was found. A phase III trial investigated the efficacy of PD-1 inhibitors combined with carboplatin + paclitaxel versus that of carboplatin

Table 4 Intraobserver and interobserver correlation coefficients for baseline myocardial work indices.

Variables	Intraobserver			Interobserver		
	ICC	95% CI	P value	ICC	95% CI	P value
GWI	0.954	0.891–0.982	<0.001	0.937	0.850–0.974	<0.001
GCW	0.990	0.975–0.996	<0.001	0.961	0.903–0.984	<0.001
GWW	0.965	0.914–0.986	<0.001	0.982	0.954–0.993	<0.001
GWE	0.952	0.882–0.981	<0.001	0.979	0.948–0.992	<0.001

ICC, intraclass correlation; CI, confidence interval; GWI, global work index; GCW, global constructive work; GWW, global wasted work; GWE, global work efficiency.

Table 5 Associations between disease characteristics and myocardial work indices

Variables	Tumor type		Treatment regimen		Cardiovascular risk factors		Cardiovascular drugs		irAEs	
	F	P value	F	P value	F	P value	F	P value	F	P value
PSD	0.372	0.545	0.437	0.648	0.615	0.545	0.004	0.950	2.388	0.080
GLS	0.868	0.356	1.212	0.306	0.353	0.705	0.124	0.726	3.314	0.034
GWI	3.937	0.053	0.767	0.470	1.060	0.354	0.884	0.352	1.746	0.170
GCW	2.547	0.117	0.407	0.668	1.234	0.300	3.936	0.053	1.227	0.310
GWW	0.061	0.805	0.406	0.668	0.409	0.667	0.209	0.650	18.614	<0.001
GWE	0.252	0.618	0.461	0.633	0.235	0.792	0.024	0.878	20.224	<0.001

PSD, peak strain dispersion; GLS, global longitudinal strain; GWI, global work index; GCW, global constructive work; GWW, global wasted work; GWE, global work efficiency; irAE, immune-related adverse event.

+ paclitaxel alone in the treatment of lung cancer. No difference in the incidence of CAEs between ICIs combined with chemotherapy and ICIs alone was found (33). Furthermore, we discovered that tumor type, cardiovascular risk factors, and cardiovascular drugs had no influence on myocardial work indices. This result was similar to previous findings, which showed the use of cardioprotective drugs to not be associated with the occurrence of CAEs (34). During the follow-up, some patients developed different numbers of irAEs during PD-1 inhibitor therapy. Specifically, LV systolic function was significantly impaired in patients with 2 and 3 irAEs, and GLS, GWW, and GWE were no longer in the normal reference range during T1 and T2. In previous research on ICIs-related myocarditis, most patients had several irAEs, including a rash, fever, renal insufficiency, hepatitis, colitis, and a combination of myasthenia gravis and myositis, which might have occurred due to the cardiac and skeletal muscles having common T-cell antigens (35,36). Therefore, the presence of 2 or more irAEs during PD-1 inhibitor therapy may help clinicians to be alert to ICIs-related cardiac injury.

A retrospective study showed that GLS might contribute to the diagnosis and prognosis of ICIs-related CAEs, with GLS being significantly lower in patients with CAE than in normal controls (37). However, GLS is limited by changes in hemodynamic conditions and cannot reflect myocardial metabolism and energy utilization. Noninvasive myocardial work is a new technology that indirectly reflects myocardial performance and oxygen consumption. Studies have shown that this technology benefits clinical practice and can detect LV functional abnormalities at an early stage (16,38).

Noninvasive myocardial work represents significant progress in the diagnosis and treatment of cardiovascular diseases (39-41). Some studies have suggested that noninvasive myocardial work is superior to GLS in predicting results and detecting coronary heart disease and may find subclinical diseases that GLS cannot show (26,42,43). At the end of 4 treatment cycles, although there were significant changes in GLS, PSD, GWI, and GCW compared with T0, the indices remained at normal reference

Table 6 Influences of irAEs on the changes of GLS, GWW, and GWE

irAEs	Treatment cycles				
	T0	T1	T2	T3	T4
GLS (%)					
None	−20.19±1.08	−19.90±1.30	−19.55±1.50	−19.51±1.41	−19.39±1.28
One	−20.80±1.40	−20.10±1.79	−19.50±1.27	−19.70±1.33	−19.60±1.35
Two	−20.63±1.41	−19.13±1.96	−18.63±2.72	−18.37±2.33	−18.00±2.27
Three	−20.67±0.58	−17.33±0.58	−16.67±0.58	−16.67±0.58	−16.33±0.58
GWW (mmHg%)					
None	82.00±19.51	102.52±15.29	127.32±23.27	119.65±17.64	122.45±17.29
One	65.10±15.41	93.20±9.89	125.80±24.73	154.30±30.95	145.90±31.00
Two	80.13±16.81	135.38±89.91	147.75±43.24	192.00±88.07	200.88±58.52
Three	75.33±19.35	190.33±13.28	247.00±33.87	263.00±45.03	247.33±45.37
GWE (%)					
None	96.16±1.07	94.94±0.89	93.32±1.60	93.71±1.04	93.45±1.15
One	97.00±0.94	95.30±0.48	93.40±1.26	92.10±1.85	92.20±1.40
Two	96.00±1.31	93.13±4.05	91.63±2.56	89.38±5.10	89.13±2.85
Three	96.33±0.58	90.00±0.14	87.33±2.08	85.00±1.00	87.33±0.58

Data are presented as the mean ± standard deviation. GLS, global longitudinal strain; GWW, global wasted work; GWE, global work efficiency; irAE, immune-related adverse event.
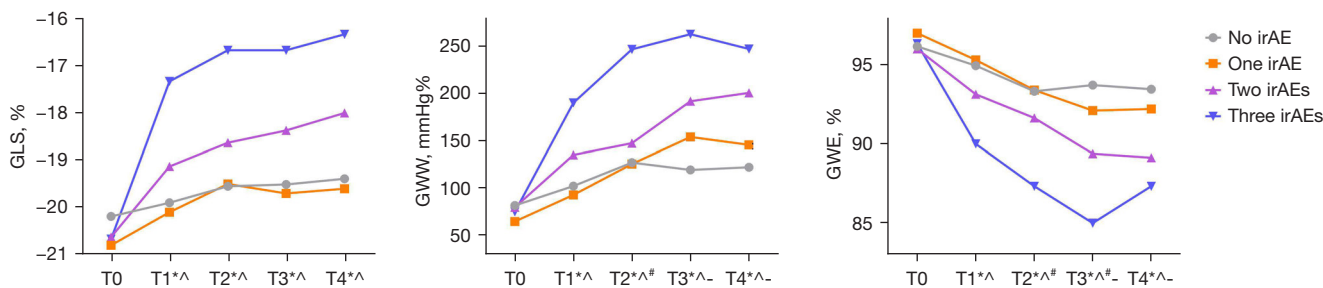

Figure 4 The trends of GLS, GWW, and GWE in different numbers of irAEs. *, the difference between 3 irAEs and 0 irAE is statistically significant; ^, the difference between 3 irAEs and 2 irAEs is statistically significant; #, the difference between 3 irAEs and 1 irAE is statistically significant; -, the difference between 2 irAEs and 0/1 irAE is statistically significant. GLS, global longitudinal strain; GWW, global wasted work; GWE, global work efficiency; irAE, immune-related adverse event.

ranges. GWW and GWE were not in the normal reference range, indicating that patients had abnormal myocardial energy metabolism. This finding may be attributable to the blockade of the PD-1/PD-L1 pathway by PD-1 inhibitors resulting in the overactivation of T cells. Not only does overactivated T cells infiltrate cardiac myocytes,

but also they release tumor necrosis factor-α, granzyme B, and interferon-γ, which induce cardiac myocytes death and myocardial damage (44-46). Moreover, the changes in cardiac function parameters were minimal throughout the follow-up period, which may be related to the absence of adverse effects in most patients, and the vast majority

of patients had a normal cardiac function. Fortunately, it has been shown that patients with ICIs-related CAEs do not experience CAE recurrence (18). The probability of complete reversal of LV systolic dysfunction in patients with mild CAEs may be as high as 50%. Therefore, early detection of cardiac insufficiency in patients treated with PD-1 inhibitors is essential to preventing irreversible cardiac dysfunction and reducing mortality and morbidity.

The present study has several limitations. First, the use of a single-center design is associated with various types of bias. A multicenter study is thus needed to validate the value of noninvasive myocardial work for monitoring ICIs-related cardiotoxicity. Second, this study lacked long-term follow-up to predict delayed adverse cardiac events and to assess whether adverse cardiac events were associated with dose accumulation. Furthermore, the time, group effects, and interaction effects of irAEs on GLS, GWW, and GWE were not reported. Finally, alcohol, diabetes, food intake, respiration timing, and conditioning might have affected myocardial work indices but were not accounted for. The above issues should be considered in future studies.

Conclusions

In conclusion, noninvasive myocardial work enables a good understanding of the myocardial function and energy utilization in patients with advanced lung cancer with PD-1 inhibitor treatment. Patients with 2 or more irAEs during PD-1 inhibitor therapy may be more prone to abnormal LV systolic function. Noninvasive myocardial work may benefit the management of patients with ICIs-related cardiotoxicity.

Acknowledgments

Footnote

Reporting Checklist: The authors have completed the STROBE reporting checklist. Available at https://qims.amegroups.com/article/view/10.21037/qims-22-817/rc

Conflicts of Interest: All authors have completed the ICMJE uniform disclosure form (available at https://qims.amegroups.com/article/view/10.21037/qims-22-817/coif). All authors report that the study receives the support from the Key Science and Technology Research Project of the Department of Education (No. GJJ190002) and the Science and Technology Program of the Health Care Commission in Jiangxi (No. 20201053). The authors have no other conflicts of interest to declare.

Ethical Statement: The authors are accountable for all aspects of the work in ensuring that questions related to the accuracy or integrity of any part of the work are appropriately investigated and resolved. The study was conducted in accordance with the Declaration of Helsinki (as revised in 2013) and was approved by the Ethics Committee of the Second Affiliated Hospital of Nanchang University (No. 20220718034425258). Informed consent was obtained from all participants.

References

1. Vaddepally RK, Kharel P, Pandey R, Garje R, Chandra AB. Review of Indications of FDA-Approved Immune Checkpoint Inhibitors per NCCN Guidelines with the Level of Evidence. Cancers (Basel) 2020;12:738.

2. Larkin J, Chiarion-Sileni V, Gonzalez R, Grob JJ, Cowey CL, Lao CD, et al. Combined Nivolumab and Ipilimumab or Monotherapy in Untreated Melanoma. N Engl J Med 2015;373:23-34.

3. Vokes EE, Ready N, Felip E, Horn L, Burgio MA, Antonia SJ, et al. Nivolumab versus docetaxel in previously treated advanced non-small-cell lung cancer (CheckMate 017 and CheckMate 057): 3-year update and outcomes in patients with liver metastases. Ann Oncol 2018;29:959-65.

4. Kim H, Kim DW, Kim M, Lee Y, Ahn HK, Cho JH, Kim IH, Lee YG, Shin SH, Park SE, Jung J, Kang EJ, Ahn MJ. Long-term outcomes in patients with advanced and/ or metastatic non-small cell lung cancer who completed 2 years of immune checkpoint inhibitors or achieved a

durable response after discontinuation without disease progression: Multicenter, real-world data (KCSG LU20-11). Cancer 2022;128:778-87.

5. Weber JS, Kähler KC, Hauschild A. Management of immune-related adverse events and kinetics of response with ipilimumab. J Clin Oncol 2012;30:2691-7.

6. Socinski MA, Jotte RM, Cappuzzo F, Orlandi F, Stroyakovskiy D, Nogami N, et al. Atezolizumab for First-Line Treatment of Metastatic Nonsquamous NSCLC. N Engl J Med 2018;378:2288-301.

7. Dougan M, Pietropaolo M. Time to dissect the autoimmune etiology of cancer antibody immunotherapy. J Clin Invest 2020;130:51-61.

8. Zhou J, Lee S, Lakhani I, Yang L, Liu T, Zhang Y, Xia Y, Wong WT, Bao KKH, Wong ICK, Tse G, Zhang Q. Adverse Cardiovascular Complications following prescription of programmed cell death 1 (PD-1) and programmed cell death ligand 1 (PD-L1) inhibitors: a propensity-score matched Cohort Study with competing risk analysis. Cardiooncology 2022;8:5.

9. Wang DY, Salem JE, Cohen JV, Chandra S, Menzer C, Ye F, et al. Fatal Toxic Effects Associated With Immune Checkpoint Inhibitors: A Systematic Review and Meta-analysis. JAMA Oncol 2018;4:1721-8.

10. D'Souza M, Nielsen D, Svane IM, Iversen K, Rasmussen PV, Madelaire C, Fosbøl E, Køber L, Gustafsson F, Andersson C, Gislason G, Torp-Pedersen C, Schou M. The risk of cardiac events in patients receiving immune checkpoint inhibitors: a nationwide Danish study. Eur Heart J 2021;42:1621-31.

11. Plana JC, Galderisi M, Barac A, Ewer MS, Ky B, Scherrer-Crosbie M, et al. Expert consensus for multimodality imaging evaluation of adult patients during and after cancer therapy: a report from the American Society of Echocardiography and the European Association of Cardiovascular Imaging. Eur Heart J Cardiovasc Imaging 2014;15:1063-93.

12. Sawaya H, Sebag IA, Plana JC, Januzzi JL, Ky B, Tan TC, Cohen V, Banchs J, Carver JR, Wiegers SE, Martin RP, Picard MH, Gerszten RE, Halpern EF, Passeri J, Kuter I, Scherrer-Crosbie M. Assessment of echocardiography and biomarkers for the extended prediction of cardiotoxicity in patients treated with anthracyclines, taxanes, and trastuzumab. Circ Cardiovasc Imaging 2012;5:596-603.

13. Negishi K, Negishi T, Hare JL, Haluska BA, Plana JC, Marwick TH. Independent and incremental value of deformation indices for prediction of trastuzumab-induced cardiotoxicity. J Am Soc Echocardiogr 2013;26:493-8.

14. Liu F, Wang X, Liu D, Zhang C. Frequency and risk factors of impaired left ventricular global longitudinal strain in patients with end-stage renal disease: a two-dimensional speckle-tracking echocardiographic study. Quant Imaging Med Surg 2021;11:2397-405.

15. Burns AT, La Gerche A, D'hooge J, MacIsaac AI, Prior DL. Left ventricular strain and strain rate: characterization of the effect of load in human subjects. Eur J Echocardiogr 2010;11:283-9.

16. Russell K, Eriksen M, Aaberge L, Wilhelmsen N, Skulstad H, Remme EW, Haugaa KH, Opdahl A, Fjeld JG, Gjesdal O, Edvardsen T, Smiseth OA. A novel clinical method for quantification of regional left ventricular pressure-strain loop area: a non-invasive index of myocardial work. Eur Heart J 2012;33:724-33.

17. Aalen JM, Donal E, Larsen CK, Duchenne J, Lederlin M, Cvijic M, Hubert A, Voros G, Leclercq C, Bogaert J, Hopp E, Fjeld JG, Penicka M, Linde C, Aalen OO, Kongsgård E, Galli E, Voigt JU, Smiseth OA. Imaging predictors of response to cardiac resynchronization therapy: left ventricular work asymmetry by echocardiography and septal viability by cardiac magnetic resonance. Eur Heart J 2020;41:3813-23.

18. Yu L, Xu AQ, Hu HL. Effect of PD-1/PD-L1 immune checkpoint inhibitors on right ventricular function. Chinese Journal of Clinical Medicine 2021;28:152-8.

19. Escudier M, Cautela J, Malissen N, Ancedy Y, Orabona M, Pinto J, Monestier S, Grob JJ, Scemama U, Jacquier A, Lalevee N, Barraud J, Peyrol M, Laine M, Bonello L, Paganelli F, Cohen A, Barlesi F, Ederhy S, Thuny F. Clinical Features, Management, and Outcomes of Immune Checkpoint Inhibitor-Related Cardiotoxicity. Circulation 2017;136:2085-7.

20. Dolladille C, Ederhy S, Allouche S, Dupas Q, Gervais R, Madelaine J, Sassier M, Plane AF, Comoz F, Cohen AA, Thuny FR, Cautela J, Alexandre J. Late cardiac adverse events in patients with cancer treated with immune checkpoint inhibitors. J Immunother Cancer 2020.

21. Vesper HW, Myers GL, Miller WG. Current practices and challenges in the standardization and harmonization of clinical laboratory tests. Am J Clin Nutr 2016;104 Suppl 3:907S-12S.

22. Lang RM, Badano LP, Mor-Avi V, Afilalo J, Armstrong A, Ernande L, Flachskampf FA, Foster E, Goldstein SA, Kuznetsova T, Lancellotti P, Muraru D, Picard MH, Rietzschel ER, Rudski L, Spencer KT, Tsang W, Voigt JU. Recommendations for cardiac chamber quantification by echocardiography in adults: an update from the

American Society of Echocardiography and the European Association of Cardiovascular Imaging. J Am Soc Echocardiogr 2015;28:1-39.e14.

23. Smiseth OA, Donal E, Penicka M, Sletten OJ. How to measure left ventricular myocardial work by pressure-strain loops. Eur Heart J Cardiovasc Imaging 2021;22:259-61.

24. Li X, Chen H, Han M, Luo Y, Liu F, Chen L, Wang X, Zhao Y, Kang R, Wang C, Zhang C. Quantitative assessment of left ventricular systolic function in patients with systemic lupus erythematosus: a non-invasive pressure-strain loop technique. Quant Imaging Med Surg 2022;12:3170-83.

25. Meucci MC, Butcher SC, Galloo X, van der Velde ET, Marsan NA, Bax JJ, Delgado V. Noninvasive Left Ventricular Myocardial Work in Patients with Chronic Aortic Regurgitation and Preserved Left Ventricular Ejection Fraction. J Am Soc Echocardiogr 2022;35:703-711.e3.

26. Manganaro R, Marchetta S, Dulgheru R, Ilardi F, Sugimoto T, Robinet S, et al. Echocardiographic reference ranges for normal non-invasive myocardial work indices: results from the EACVI NORRE study. Eur Heart J Cardiovasc Imaging 2019;20:582-90.

27. Papadopoulos K, Özden Tok Ö, Mitrousi K, Ikonomidis I. Myocardial Work: Methodology and Clinical Applications. Diagnostics (Basel) 2021.

28. Mahmood SS, Fradley MG, Cohen JV, Nohria A, Reynolds KL, Heinzerling LM, Sullivan RJ, Damrongwatanasuk R, Chen CL, Gupta D, Kirchberger MC, Awadalla M, Hassan MZO, Moslehi JJ, Shah SP, Ganatra S, Thavendiranathan P, Lawrence DP, Groarke JD, Neilan TG. Myocarditis in Patients Treated With Immune Checkpoint Inhibitors. J Am Coll Cardiol 2018;71:1755-64.

29. Martins F, Sofiya L, Sykiotis GP, Lamine F, Maillard M, Fraga M, Shabafrouz K, Ribi C, Cairoli A, Guex-Crosier Y, Kuntzer T, Michielin O, Peters S, Coukos G, Spertini F, Thompson JA, Obeid M. Adverse effects of immune-checkpoint inhibitors: epidemiology, management and surveillance. Nat Rev Clin Oncol 2019;16:563-80.

30. Wang F, Sun X, Qin S, Hua H, Liu X, Yang L, Yang M. A retrospective study of immune checkpoint inhibitor-associated myocarditis in a single center in China. Chin Clin Oncol 2020;9:16.

31. Tarrio ML, Grabie N, Bu DX, Sharpe AH, Lichtman AH. PD-1 protects against inflammation and myocyte damage in T cell-mediated myocarditis. J Immunol 2012;188:4876-84.

32. Nishimura H, Okazaki T, Tanaka Y, Nakatani K, Hara M, Matsumori A, Sasayama S, Mizoguchi A, Hiai H, Minato N, Honjo T. Autoimmune dilated cardiomyopathy in PD-1 receptor-deficient mice. Science 2001;291:319-22.

33. Paz-Ares L, Luft A, Vicente D, Tafreshi A, Gümüş M, Mazières J, et al. Pembrolizumab plus Chemotherapy for Squamous Non-Small-Cell Lung Cancer. N Engl J Med 2018;379:2040-51.

34. Lal JC, Brown SA, Collier P, Cheng F. A retrospective analysis of cardiovascular adverse events associated with immune checkpoint inhibitors. Cardiooncology 2021;7:19.

35. Ansari-Gilani K, Tirumani SH, Smith DA, Nelson A, Alahmadi A, Hoimes CJ, Ramaiya NH. Myocarditis associated with immune checkpoint inhibitor therapy: a case report of three patients. Emerg Radiol 2020;27:455-60.

36. Esfahani K, Buhlaiga N, Thébault P, Lapointe R, Johnson NA, Miller WH Jr. Alemtuzumab for Immune-Related Myocarditis Due to PD-1 Therapy. N Engl J Med 2019;380:2375-6.

37. Awadalla M, Mahmood SS, Groarke JD, Hassan MZO, Nohria A, Rokicki A, et al. Global Longitudinal Strain and Cardiac Events in Patients With Immune Checkpoint Inhibitor-Related Myocarditis. J Am Coll Cardiol 2020;75:467-78.

38. Boe E, Russell K, Eek C, Eriksen M, Remme EW, Smiseth OA, Skulstad H. Non-invasive myocardial work index identifies acute coronary occlusion in patients with non-ST-segment elevation-acute coronary syndrome. Eur Heart J Cardiovasc Imaging 2015;16:1247-55.

39. Galli E, Leclercq C, Hubert A, Bernard A, Smiseth OA, Mabo P, Samset E, Hernandez A, Donal E. Role of myocardial constructive work in the identification of responders to CRT. Eur Heart J Cardiovasc Imaging 2018;19:1010-8.

40. Huang D, Cui C, Zheng Q, Li Y, Liu Y, Hu Y, Wang Y, Liu R, Liu L. Quantitative Analysis of Myocardial Work by Non-invasive Left Ventricular Pressure-Strain Loop in Patients With Type 2 Diabetes Mellitus. Front Cardiovasc Med 2021;8:733339.

41. Hiemstra YL, van der Bijl P, El Mahdiui M, Bax JJ, Delgado V, Marsan NA. Myocardial Work in Nonobstructive Hypertrophic Cardiomyopathy: Implications for Outcome. J Am Soc Echocardiogr 2020;33:1201-8.

42. Edwards NFA, Scalia GM, Shiino K, Sabapathy S, Anderson B, Chamberlain R, Khandheria BK, Chan J. Global Myocardial Work Is Superior to Global

Longitudinal Strain to Predict Significant Coronary Artery Disease in Patients With Normal Left Ventricular Function and Wall Motion. J Am Soc Echocardiogr 2019;32:947-57.

43. Liu FZ, Wang XL, Zhang CQ. Quantitative assessment of left ventricular myocardial work in chronic kidney disease patients by a novel non-invasive pressure-strain loop analysis method. Int J Cardiovasc Imaging 2021;37:1567-75.

44. Patel RP, Parikh R, Gunturu KS, Tariq RZ, Dani

SS, Ganatra S, Nohria A. Cardiotoxicity of Immune Checkpoint Inhibitors. Curr Oncol Rep 2021;23:79.

45. Tocchetti CG, Galdiero MR, Varricchi G. Cardiac Toxicity in Patients Treated With Immune Checkpoint Inhibitors: It Is Now Time for Cardio-Immuno-Oncology. J Am Coll Cardiol 2018;71:1765-7.

46. Johnson DB, Balko JM, Compton ML, Chalkias S, Gorham J, Xu Y, et al. Fulminant Myocarditis with Combination Immune Checkpoint Blockade. N Engl J Med 2016;375:1749-55.